

# ***In vivo* performance of innovative polyelectrolyte matrices for hot melt extrusion of amorphous drug systems**

Felix Ditzinger <sup>1,2</sup>, Rebecca Wieland <sup>1</sup>, Marina Statelova <sup>3</sup>, Maria Vertzoni <sup>3</sup>, René Holm <sup>4,5</sup>, Martin  
Kuentz <sup>2,\*</sup>

<sup>1</sup> Department of Pharmaceutical Sciences, University of Basel, 4056 Basel, Switzerland

<sup>2</sup> Institute of Pharma Technology, University of Applied Sciences and Arts Northwestern Switzerland,  
4132 Muttenz, Switzerland

<sup>3</sup> Department of Pharmacy, National and Kapodistrian University of Athens, 157 72 Athens, Greece

<sup>4</sup> Drug Product Development, Janssen Research and Development, Johnson and Johnson, 2340 Beerse,  
Belgium

<sup>5</sup> Department of Science and Environment, Roskilde University, 4000 Roskilde, Denmark

## **Corresponding author:**

Prof. Dr. Martin Kuentz

University of Applied Sciences and Arts Northwestern Switzerland

Institute of Pharma Technology

Hofackerstr. 30

4132 Muttenz, Switzerland

Phone number: 0041 61 228 56 42

[martin.kuentz@fhnw.ch](mailto:martin.kuentz@fhnw.ch)

## Abstract

Hot melt extrusion of amorphous systems has become a pivotal technology to cope with challenges of poorly water-soluble drugs. Previous research showed that small-molecular additives with targeted molecular interactions enabled introduction of a polyelectrolyte matrix to hot melt extrusion that would be otherwise not possible to process due to the unfavorable melting properties of the pure polymer. Carboxymethyl cellulose (NaCMC) with lysine or alternatively meglumine was leading to modified polymeric matrices that showed adequate processability by hot melt extrusion and yielded stable amorphous formations. The investigated formulations, including fenofibrate as a model drug, were characterized by attenuated total reflectance Fourier transform infrared spectroscopy, differential scanning calorimetry, as well as viscosity measurements after aqueous dispersion. Further biopharmaceutical assessment started with biorelevant non-sink dissolution testing followed by a pharmacokinetic *in vivo* study in rats. The *in vitro* assessment showed superiority of the lysine containing formulation in the extent of *in vitro* supersaturation and overall drug release. In accordance with this, the *in vivo* study also demonstrated increased exposure of the amorphous formulations and in particular for the system containing lysine. In summary, the combination of polyelectrolytes with interacting additives presents a promising opportunity for the formulation of poorly water-soluble drugs.

## 1. Introduction

The challenge of improving the bioavailability of poorly water-soluble drugs is a crucial aspect that pharmaceutical experts have to cope with throughout modern pharmaceutical development. An approach, which has gained popularity in the recent decade, is the formulation of drug in an amorphous form. Such a formulation approach typically leads to an apparent solubility increase and hence drug supersaturation upon dispersion after oral administration<sup>1</sup>. A high level of stabilized supersaturation in the small intestine results in enhanced bioavailability of orally delivered drugs<sup>2,3</sup>. Especially enabling formulations like amorphous systems processed by hot melt extrusion (HME) are capable of enhancing the supersaturation of BCS (i.e. biopharmaceutics classification system) class II drugs like fenofibrate (FE) to an extent that the absorption upon oral administration can become comparable to that of a BCS class I drug<sup>4</sup>. The assessment of such drug supersaturation is ideally performed under non-sink conditions using biorelevant media<sup>5-7</sup>. Since the supersaturation potential is dependent on the amorphous stability of the drug in the solid state<sup>8,9</sup>, a combination of this assay with a stability-based comparison of supersaturation capabilities is applied in the so-called screening of polymers for amorphous drug stabilization (SPADS) approach, which is a screening method applied in the pharmaceutical industry for polymer selection during the development of amorphous solid dispersions (ASDs)<sup>10</sup>.

Polymers with high molecular weight often affect drug precipitation following dispersion by a decrease of molecular mobility<sup>11</sup>. Such polymers can inhibit nucleation and/or growth as it was for example shown for the active pharmaceutical ingredient (API) indomethacin<sup>12</sup> and a variety of commonly used pharmaceutical polymers<sup>13</sup>. The functionality of polymers to act as precipitation inhibitors in solution is crucial in a supersaturating formulation<sup>11,14,15</sup>. An example of such a stabilizing polymer is the polyelectrolyte sodium carboxymethyl cellulose (NaCMC). Polyelectrolytes are commonly used as superdisintegrants in conventional solid dosage forms or they can find application as ionic liquids, where the combination of ionically interacting substances may lead to benefits in a pharmaceutical dosage form<sup>16</sup>. For the latter application, the intense swelling of superdisintegrants leads to faster disintegration of the solid dosage form, which would also be beneficial in a polymeric ASD but should be balanced with a risk of precipitation because of a too fast drug release<sup>11,17</sup>.

In particular, NaCMC showed attractive stabilization of supersaturated drug<sup>18</sup> and an increase in overall oral bioavailability<sup>19</sup>. One factor might be the viscosity increase as stabilization of a supersaturated drug<sup>20,21</sup>. Even before drug gets entirely into solution, a polymer such as NaCMC could exert stabilizing effects in contact with aqueous media. Most recently, Edueng and colleagues identified the need of understanding the influence of the viscous interface between amorphous material and water on nucleation kinetics<sup>22</sup>.

Unfortunately, the polyelectrolyte NaCMC is not applicable for HME in the neat form due to its high melting point and thermal degradation at the required processing temperature<sup>23</sup>. Therefore, the principle of molecularly interacting conformers<sup>24</sup> was investigated with a new focus of changing polymer properties rather than targeting direct drug-additive interactions<sup>25,26</sup>. In case of polyelectrolyte NaCMC, it was possible to obtain an extrudable polymeric matrix of the polyelectrolyte and a stable glass formation was

demonstrated by means of synchrotron powder X-ray diffraction<sup>25</sup>. Although this recent work identified meglumine (Meg) and lysine (Lys) as most suitable co-formers in the applied dataset, a biopharmaceutical assessment with an *in vivo* study have not yet been conducted to support the potential of the new approach. The present study therefore used the identified polyelectrolyte matrices to incorporate FE as a poorly water-soluble model drug, because it is known to precipitate rapidly from supersaturated solution and its stabilization by excipients was found to be difficult<sup>27</sup>.

In this study, the solid dispersions were developed with regards to a drug load that provided completely amorphous formulations. The amorphous form of FE in both formulations was evaluated by differential scanning calorimetry (DSC) and powder X-ray diffraction (PXRD). Regarding drug release testing, the two formulations were compared with their corresponding physical mixtures in a non-sink fasted simulated intestinal fluid (FaSSIF) dissolution experiment<sup>6,7</sup>. To gain further insights in the stabilization properties of NaCMC, viscosity measurements were performed. For a better correlation with the performed dissolution experiments, the viscosity was measured in FaSSIF after the duration of the dissolution experiments. Moreover, the formulations and their physical mixtures were investigated in a pharmacokinetic (PK) study in rats to investigate the viability of the approach using NaCMC amorphous formulations produced by HME and FE as a model compound.

## **2. Materials and Methods**

### **2.1 Materials**

FE, NaCMC (low viscosity), Lys and Meg were bought from Sigma-Aldrich (Bruchs, Switzerland). SIF powder for FaSSIF media was bought from biorelevant.com (Biorelevant.com Ltd, London, UK). Purified water for the viscosity measurements as well as the dissolution media was taken from a MilliQ Millipore filter system (Millipore Co., Bedford, MA, USA). All solvents for the UPLC analysis were of LC-MS quality and bought from Sigma Aldrich (Bruchs, Switzerland). Filters and other consumables were bought from Sigma-Aldrich (Bruchs, Switzerland).

### **2.2 Methods**

#### **2.2.1 Preparation of hot melt extrudates**

Binary mixtures of NaCMC and Meg or Lys in a ratio of 50/50 % (w/w) were mixed in a mortar and dissolved in MilliQ water in a round bottom flask. Afterwards, the water was removed by a rotary evaporator (Rotavapor Büchi, Flawil, Switzerland). The resulting film was cut into smaller pieces and ground in a mortar. This powder was mixed with FE in a ratio of 92.5/7.5 % (w/w) and extruded on a ZE9 ECO twin-screw extruder (co-rotating screws with a 9-mm diameter and 180 mm in length) by ThreeTec (Birren, Switzerland). A screw speed of 80 rpm was applied at a temperature of 130 °C through all three heating zones. The final extrudates were cooled to room temperature and stored in falcon tubes. This experimental procedure was established as previously described developing polyelectrolyte matrices<sup>25</sup>.

### 2.2.2 Powder X-ray diffraction

The extrudates were analysed by PXRD on a D2 Phaser diffractometer (Bruker AXS GmbH, Karlsruhe, Germany) with a 1-D Lynxeye detector. The instrument was equipped with a Ge-monochromator (Cu K $\alpha$  radiation) providing X-ray radiation at a wavelength of 1.541 Å. During the measurements, a voltage of 30 kV and a current of 10 mA were used. The increment and time per step were set to 0.020 ° and 1 s, respectively. The measurement  $2\theta$  angles were stretching over a range of 5° to 40°.

### 2.2.3 Differential scanning calorimetry

Samples were further assessed by a differential scanning calorimeter on a DSC 3 (Mettler Toledo, Greifensee, Switzerland). The samples were cut in small pieces and 5 to 9 mg were placed in a 40  $\mu$ L aluminum pan with a pierced lid. A heating rate of 10 °C/min from -10 °C to 140 °C was applied, while the surrounding sample cell was purged with nitrogen at 200 mL/min. Moreover, a combination of heating, cooling and heating cycles was used to fully evaluate the samples. For the assessment of the initial form, the first heating was used. The thermograms and glass transition temperatures ( $T_g$ s) were analyzed with the STARe Evaluation-Software Version 16 (Mettler Toledo, Greifensee, Switzerland). All thermograms show exothermic events as upward peaks.

### 2.2.4 Determination of thermodynamic solubility

The medium FaSSIF was prepared according to the instructions of biorelevant.com by weighing 45 mg of FaSSGF/FaSSIF/FeSSIF powder into 45 mL of phosphate buffer (pH 6.5) <sup>5</sup>. Fenofibrate (2-3mg) was transferred into a glass vial, 2 mL of FaSSIF were added and the samples were agitated at 450 rpm for 24 hours at 37 °C. The pH was checked at 24 h and adjusted with 0.1 N NaOH or 0.1 N HCl.

Samples were filtered into a quartz glass cuvette through a 0.45  $\mu$ m PTFE Whatman filter after 24 hours. Filtrates were immediately diluted with acetonitrile and water (1:4, V/V) to avoid precipitation from the saturated solution. Samples were analyzed by a UV/VIS spectrometer (Jasco, Easton, MD, USA) at 287 nm. The experiment was carried out in triplicates.

### 2.2.5 Non-sink dissolution

The amount of extrudate containing 10 mg API was transferred into a glass vial. After adding 10 mL FaSSIF, the vials were agitated at 37 °C and 450 rpm in a shaker for 2 hours <sup>14</sup>. Samples were taken at 2, 5, 10, 15, 30, 60, 90 and 120 minutes, filtered (0.45  $\mu$ m PTFE Whatman filters), diluted, and analyzed by a UV/VIS spectrometer (Jasco, Easton, MD, USA) at 287 nm. The mini-dissolution trials were conducted in duplicate for all samples.

### **2.2.6 *In vivo* bioavailability study**

For the *in vivo* pharmacokinetic study a protocol was used, which was approved by the institutional animal ethics committee in accordance with Belgian law regulating experiments on animals and in compliance with EC directive 2010/63/EU and the NIH guidelines on animal welfare. Male Sprague-Dawley rats weighing 280–320 g on the day of the experiments were purchased from Charles River Laboratories Deutschland (Sulzfeld, Germany). The animals were acclimated for a minimum of 5 days. The animals had free access to a standard rodent diet and water *ad libitum* during the study. The animals were fasted 16–20 hours before the administration and throughout the study with free access to water. The extrudates were each delivered as ground powders for their corresponding study arm. Prior to administration, the powders were suspended in FaSSIF and delivered to the animal by oral gavage at a volume of 6.25 mL/kg with a FE dose of 20 mg/kg. By individual tail vein puncture, 100  $\mu$ L blood samples were collected into tubes containing dipotassium EDTA, plasma was harvested by centrifugation for 10 min at 1000 $\times$  g, followed by separation into polypropylene tubes and immediate freezing and storage at -20  $^{\circ}$ C. Samples were taken at 0.5 h, 1 h, 2 h, 3 h, 4 h, 6 h, 8 h, 10 h, 24 h, and 28 h following oral dosing. The animals were euthanized after the experiment.

### **2.2.7 Bioanalytical Procedure**

The analysis of the plasma samples was performed according to a validated method proposed and applied by Berthelsen et al.<sup>28</sup> In short, 50  $\mu$ L of the plasma were precipitated with acetonitrile 1:4 (v/v) in an Eppendorf<sup>®</sup> tube and the mixture was placed in an ultra-sonic bath for 10 min. Subsequently, the samples were transferred and frozen for 10 min at -20  $^{\circ}$ C, followed by centrifugation at 5  $^{\circ}$ C and 17,500 rpm for 16 min. The resulting clear supernatant was transferred into a UPLC vials for further analysis.

### **2.2.8 Ultra-High Performance Liquid Chromatography (UHPLC)**

UPLC analysis was performed using a Waters ACQUITY UPLC System (Waters Corporation, MA, USA) equipped with a photodiode array detector. The separation was achieved on an Acquity UPLC BEH column C18 (2.1 x 50 mm, 1.7  $\mu$ m, Waters, MA, USA) and a guard column ACQUITY UPLC BEH column C18 VanGuard Pre-column (2.1 mm x 5 mm 130  $\text{Å}$ , 1.7  $\mu$ m) with an injection volume of 4  $\mu$ L. The column oven temperature was maintained at 55  $^{\circ}$ C. The mobile phases A and B consisted of water: trifluoroacetic acid 999:1 (V:V) and acetonitrile, respectively. The gradient method employed began by an isocratic elution at 80:20 A:B for 0.8 min, followed by a linear increase to 0:100 A:B until 3.1 min and return to 80:20 A:B at 3.2 minutes and equilibration over a runtime of 4 min at a constant flow rate of 0.6 mL/min. Chromatograms were extracted at 287 nm for FE determination. System management, data acquisition and processing were based on the Empower software package, version 7.2 (Waters, MA, USA).

### **2.2.9 Viscosity measurement of the dissolution samples**

Prior to the measurement, the samples were filtered through a 0.8  $\mu\text{m}$  mixed cellulose ester filter to eliminate all non-dissolved particles. The measurement setup was reported in previous work<sup>29</sup>.

In brief, the micro-electro-mechanical system capillary rheometer, m-VROC™ (RheoSence, San Ramon, CA), was employed to measure the viscosity of the dissolution samples. This instrument is a microfluidic slit rheometer, which enables viscosity measurements of various sample amounts. It measures the viscosity from the pressure drop of a sample as it flows through the rectangular slit. The glass syringe (Hamilton 81260 SYR 1000 mL) was loaded with sample and placed inside of the thermal block ( $37\text{ }^{\circ}\text{C} \pm 0.2$ ) of the instrument. After the stabilization of the measurement temperature, the sample was pumped through the flow channel of the chip at shear rate  $4000\text{ s}^{-1}$ . The pressure drop was detected by a sensor (cell VROC-mA10; 10K Pa full scale, 100- $\mu\text{m}$  flow channel). On the basis of these measurements the viscosity was calculated using m-VROC Control Software (RheoSence, San Ramon, CA). The measurements were performed in triplicates.

### **2.2.10 Attenuated total reflectance Fourier transform infrared spectroscopy**

The FTIR spectrometer Cary 680 (Agilent Technologies, Santa Clara, CA, USA) was used in the attenuated total reflectance mode for the determination of interactions. The scanning range of  $4000 - 600\text{ cm}^{-1}$  was selected at a resolution of  $4\text{ cm}^{-1}$ . Such measurement was used to compare the pure drug, the physical mixture and the extrudate. For the evaluation, a spectrum was extracted and evaluated by the software ACD/Spectrum Processor 2016.1.1 (Advanced Chemistry Development, Canada).

### **2.2.11 Molecular modeling and statistical analysis**

Graphical representation of molecular interactions was based on a molecular dynamics simulation in vacuum using tube models in the program suite YASARA v. 18.11.10 (YASARA Biosciences GmbH, Vienna Austria). An AMBER14 force field was employed and each molecule was first energy minimized. Sodium carboxymethylcellulose was represented as oligomer ( $n=10$ ) and was in contact with one FE molecule to roughly approximate average relative amounts. Moreover, 10 molecules of either Lys or Meg were added and the simulation was running for 1 ns at 300 K. Such molecular ratio is approximately in line with the investigated formulations.

Data from the in vivo study in rats were analyzed using non-compartmental PK analysis. Maximum drug plasma concentration ( $C_{max}$ ) values after oral dosing were extracted directly from the observed data, while area under the plasma concentration-time curve (AUC) value were calculated using the linear trapezoidal rule using Excel 2013 (Microsoft). The software StatGraphics Version 16 (Statgraphics Technologies Inc., The Plains, VA, USA) was used for all statistical calculations. For each formulation, an Analysis of the Variance (ANOVA) with a Fisher LSD post hoc test at a 95 % confidence interval was performed. A value

of  $p < 0.05$  comparing the formulations with the corresponding physical mixtures with respect to the previously mentioned pharmacokinetic responses was considered statistically significant.

### 3. Results

#### 3.1 Molecular dynamics simulation

Before preparation of the formulations, the different systems were simulated on an atomistic level for visualization and to gain some qualitative structural insights. Assuming a simplified local composition, a small-scale molecular dynamics simulation was run for 1 ns (300 K) using an AMBER14 force field. The Figures 1 and 2 show a possible configuration of how the model drug FE may qualitatively interact with the modified matrix. Figure 1 indicates that the drug is embedded in a pocket-like structure for the formulation containing Lys. Pronounced hydrogen bonding of lysine side chains with fenofibrate are possible while meglumine can only interact via weaker hydrogen bonds of hydroxyl groups that are present in the polymer. Consequently, the situation of FE appeared to be different with the system including Meg as co-former in which the drug appears to be rather attached to the surface of the modeled polymeric matrix (Figure 2). Moreover, interaction of fenofibrate with the lysine side chain are expected in the dry state as well as upon aqueous dispersion and make a difference to the before mentioned hydroxyl interactions by meglumine.

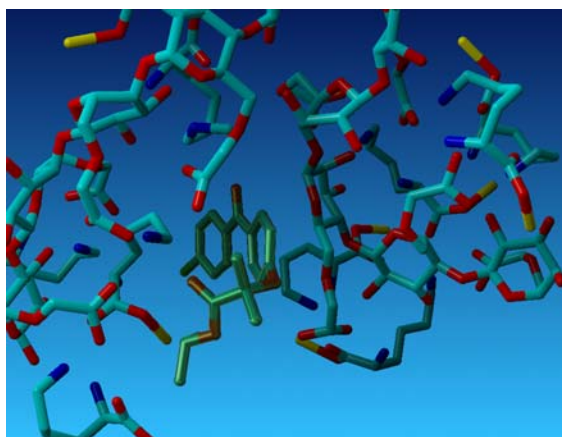


**Figure 1.** Visualization of a simplified molecular structure of the formulation Lys/NaCMC/FE based on an AMBER14 force field and 1 ns molecular dynamics simulation at 300 K (using the software YASARA <sup>30</sup>). Fenofibrate is in green, sodium ions are shown as yellow (tube model) and hydrogen bonds are represented by dashed red lines.



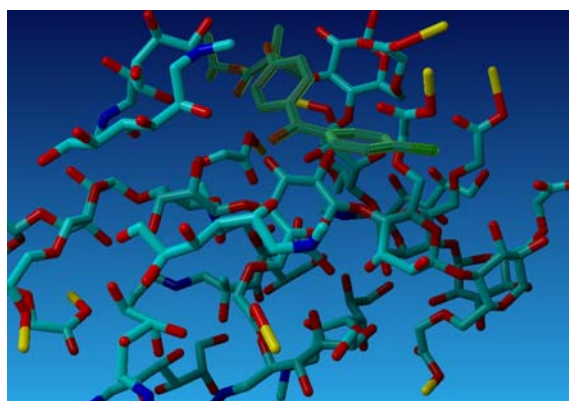


**Figure 2.** Visualization of a simplified molecular structure of the formulation Meg/NaCMC/FE based on an AMBER14 force field and 1 ns molecular dynamics simulation at 300 K (using the software YASARA<sup>30</sup>). Fenofibrate is in green, sodium ions are shown as yellow (tube model) and hydrogen bonds are represented by dashed red lines.

### 3.2 Solid-state analytics

The successful amorphization of the model drug was investigated initially by PXRD (Figure 3) as well as DSC (Figure 4.). An amorphous halo diffraction pattern was indeed obtained for the two developed formulations in comparison with the crystalline reference drug that displayed distinct Bragg peaks of the API<sup>31</sup>.

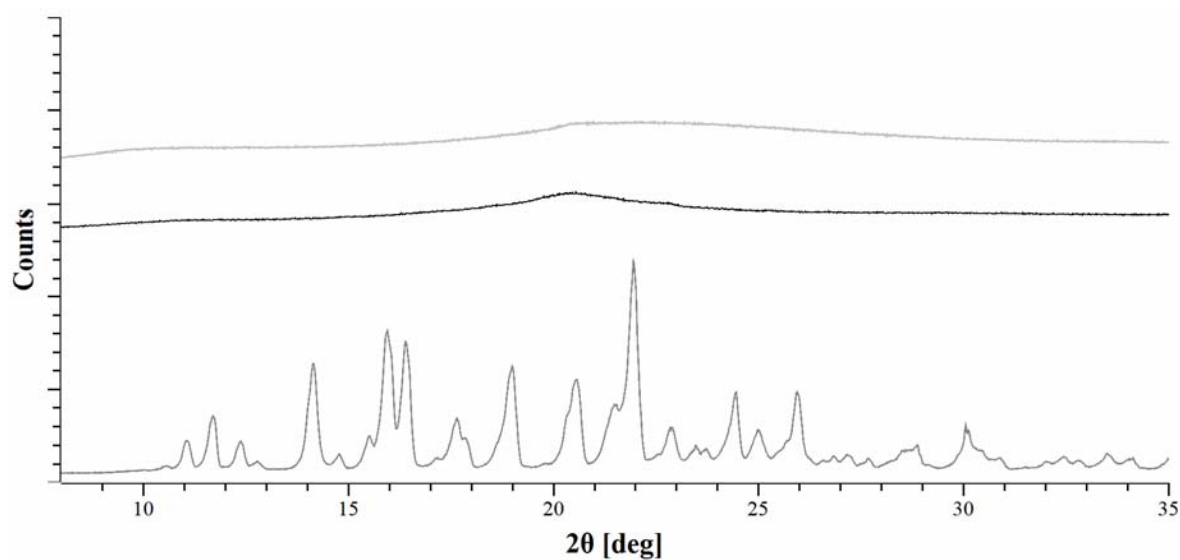


**Figure 3.** PXRD patterns of pure FE (gray, bottom), Lys/NaCMC/FE (light gray, top), Meg/NaCMC/FE (black, middle)

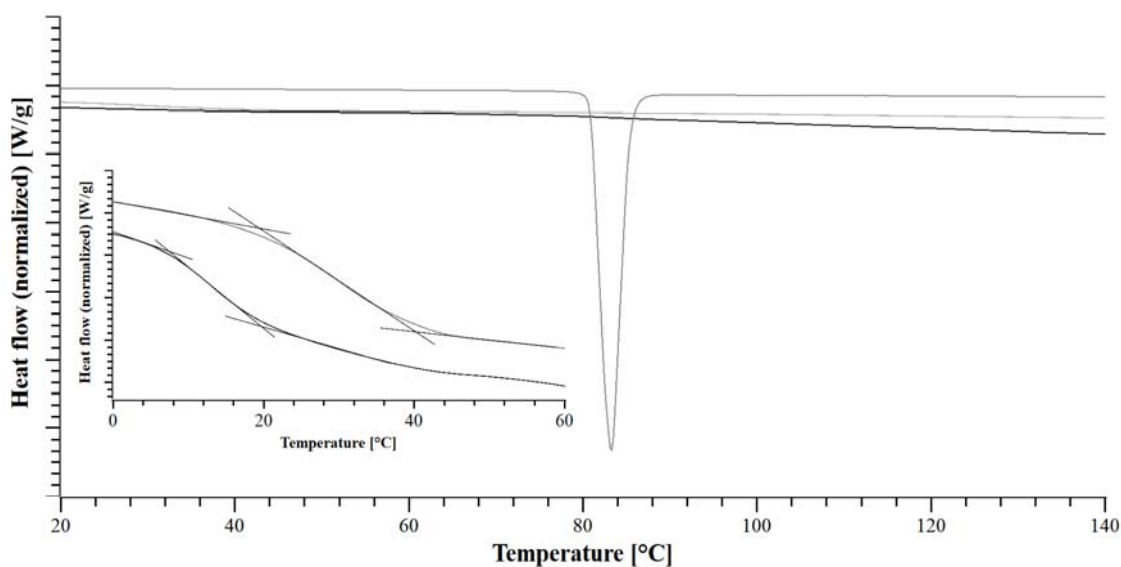


**Figure 4.** Thermograms of Lys/NaCMC/Fe (light gray,middle), Meg/NaCMC/Fe (black,bottom) and pure FE (gray,top). Insert shows  $T_g$  of Lys/NaCMC/Fe (light gray,top), Meg/NaCMC/Fe (black,bottom) in the area between 0 and 60 °C.

In the DSC thermograms, no melting peak could be detected in the formulations (Figure 4 black and light gray) in contrast to the pure model drug, which had a clear melting peak. The detected glass transitions at  $29.70 (\pm 0.20)$  °C for the Lys formulation and  $10.02 (\pm 0.82)$  °C for the Meg formulation (Figure 4 insert) were in accordance with previously performed measurements the polyelectrolyte matrices <sup>25</sup>.

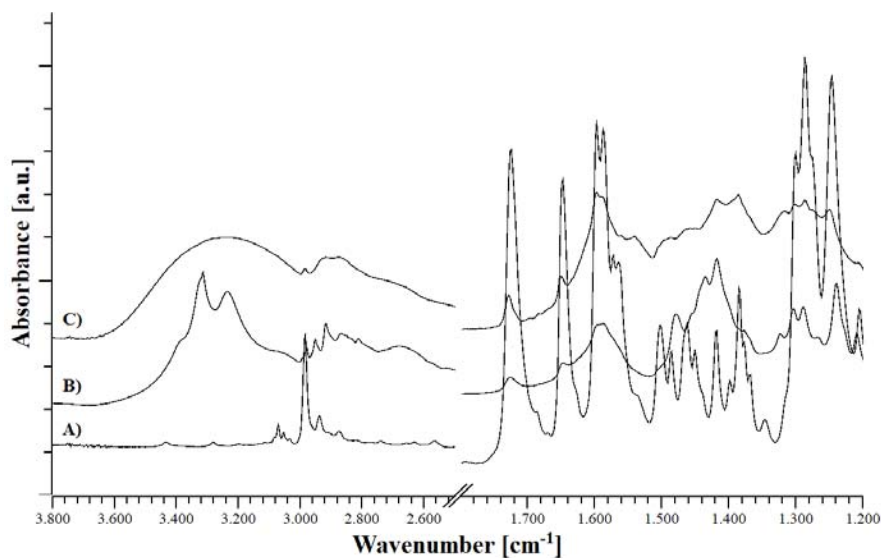


**Figure 5.** FTIR Spectrum of FE (A), Meg/NaCMC/FE physical mixture (B), Meg/NaCMC/FE extrudate (C)

The comparison of the spectra corresponding to the physical mixture, the formulation and the pure API (Figure 5) showed a significant peak broadening between the physical mixture and the formulation because

of the amorphization, which is also visible in Figure 3 and 4. This broadening is even more pronounced around  $3400\text{ cm}^{-1}$  in the area of the O-H and N-H stretching vibration of the Meg formulation.

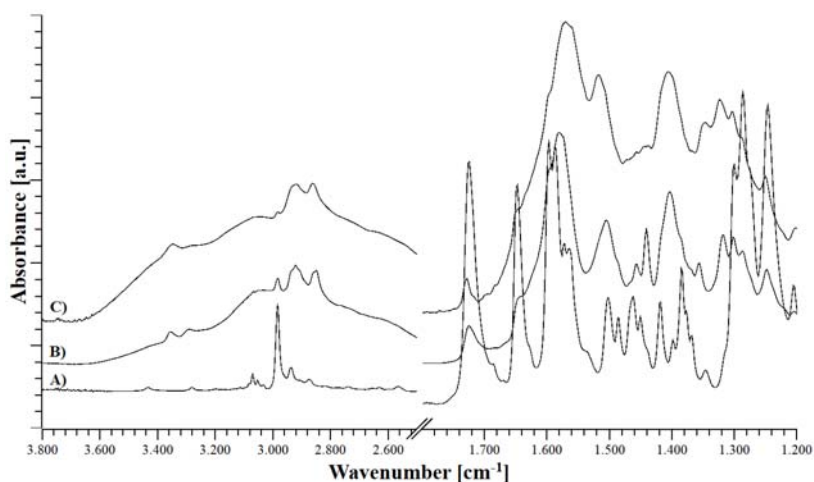


**Figure 6.** FTIR Spectrum of FE (A), Lys/NaCMC/FE physical mixture (B), Lys/NaCMC/FE extrudate (C)

In the formulation of Lys/NaCMC/FE, the amide bands at  $1572$  and  $1509\text{ cm}^{-1}$  were significantly broadened, which almost led to the formation of a combined peak (Figure 6). Moreover, the extrusion resulted in a broadening of the amine-stretching band at  $3340\text{ cm}^{-1}$ . In general, the peaks of FE were less visible in the extruded formulation.

### 3.3 Biorelevant *in vitro* dissolution study

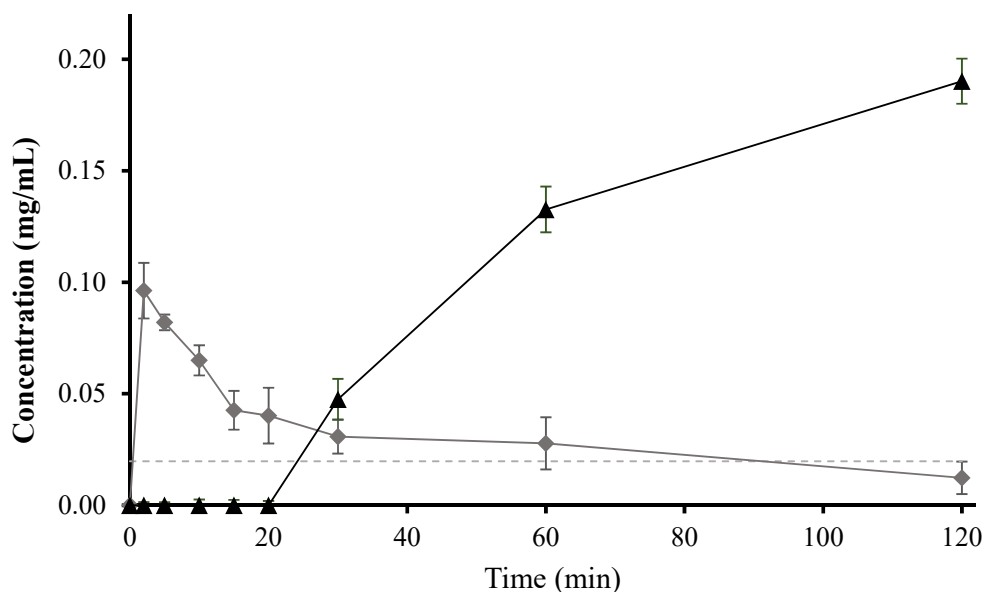


**Figure 7.** Non-sink dissolution profiles in FaSSIF of Lys/NaCMC/FE: physical mixture (gray diamonds), extruded formulation (black triangles). The dotted line represents the solubility of FE in FaSSIF.

The measured solubility of FE in FaSSIF was 0.0154 ( $\pm$  0.0005) mg/mL in agreement with current literature (Figure 7) <sup>32,33</sup>. For the physical mixture a short concentration increase can be observed at the beginning of the dissolution experiment, which was followed by a rapid decline to the thermodynamic solubility. The formulation containing Lys had a dissolution profile with a delayed release. After 30 min, the profile showed supersaturated concentrations, which were stable and increasing until 120 min. A rough estimation of the supersaturation shows about 12-fold increase, which was in line with other studies on extruded FE formulations in FaSSIF <sup>34</sup>.

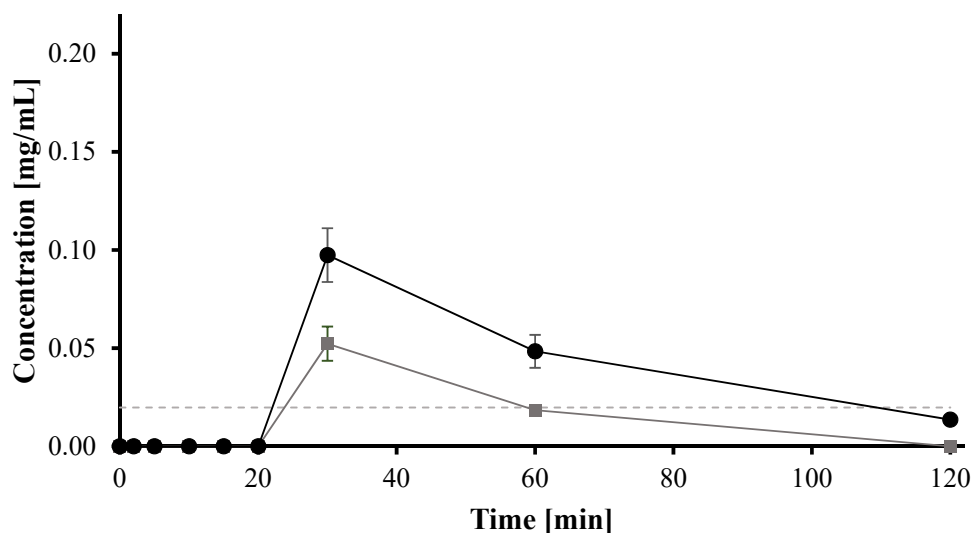


**Figure 8.** Non-sink dissolution profiles in FaSSIF of Meg/NaCMC/FE: physical mixture (gray squares), extruded formulation (black spheres). The dotted line represents the solubility of FE in FaSSIF.

The release profile of the Meg/NaCMC/FE formulation showed the identical delay in release as with the Lys formulation. Release profiles of both formulations indicated polymer swelling causing a delayed release. In contrast to the dissolution profile of Lys/NaCMC/FE, the supersaturation of Meg/NaCMC/FE is less pronounced. The overall dissolution performance was still improved in comparison to the physical mixture.

Although, the Lys/CMC/FE extrudate presented the slowest release it was the formulation, it was the systems that demonstrated the highest supersaturation and was able stabilize this state over the time of the experiment.

**Table 1.** Viscosity of the formulations and physical mixtures in FaSSIF

Composition		Viscosity <sub>2h</sub> (mPa s)
Lys, NaCMC, and FE	Formulation	3.08 ± 0.01
	Physical mixture	3.25 ± 0.07
Meg, NaCMC, and FE	Formulation	3.18 ± 0.01
	Physical mixture	2.81 ± 0.03

The dissolution study was complemented by viscosity measurements in FaSSIF at the end of the experiments. These measurements showed an increase of viscosity in all formulations and physical mixtures at the end of the study compared to the pure FaSSIF with a viscosity of 1.11 (± 0.04) mPa s (Table 1). The values among the samples did not vary greatly and highest differences were noted between the physical mixtures of the different systems.

### 3.4 *In vivo* rat study

Drug dissolution and subsequent absorption in the gastrointestinal tract of the rat resulted in high plasma levels for both formulations. The amorphous formulations generally showed faster absorption and higher concentrations than the physical mixtures. A comparison between these reference physical mixtures showed a tendency of the Lys system to provide higher exposure though not statistical significant. There was a pronounced difference between the physical mixture containing Meg and the corresponding amorphous formulation, whereas the comparison between the Lys amorphous formulation and the physical mixture was less distinct (Figure 9).

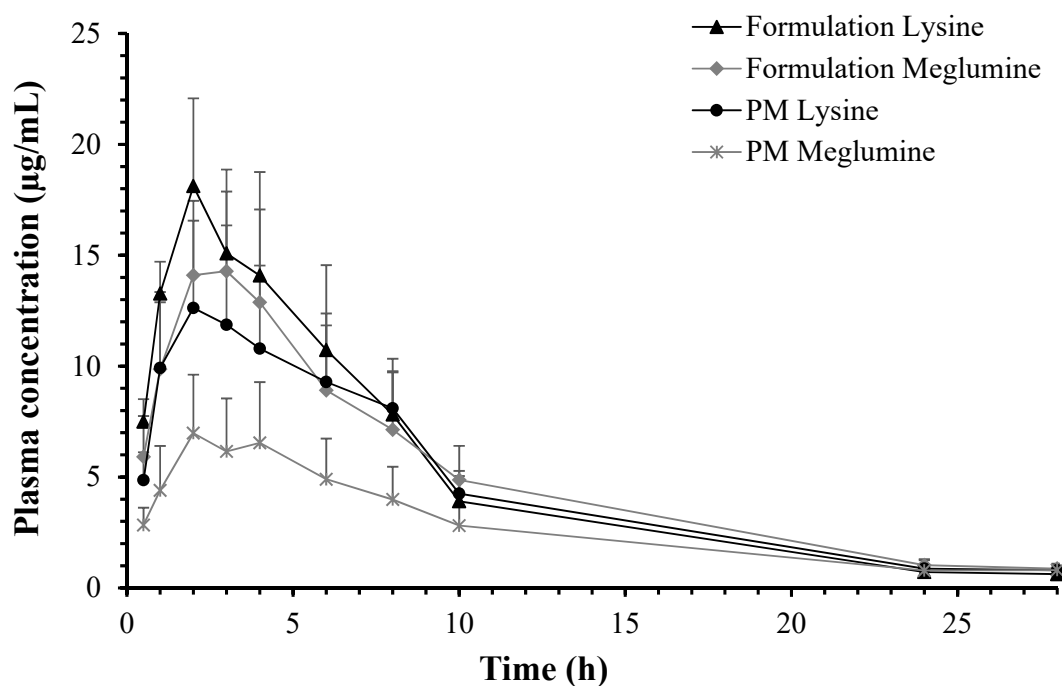


**Figure 9.** Plasma concentration (fenofibric acid) – time profile after oral administration of Lys/NaCMC/FE: physical mixture (black spheres), extruded formulation (black triangles) and Meg/NaCMC/FE: physical mixture (gray crosses), extruded formulation (gray diamonds).

For both formulations, the  $C_{max}$  values showed a statistical significant difference between the formulation and the corresponding physical mixture. Even though the  $AUC_{0-28h}$  tended to differ, only the Meg formulation showed a significant difference between the formulation and the physical mixture.

**Table 2.** Pharmacokinetic parameters of the rat study for physical mixtures and formulations of FE at 20mg/kg.

Composition		$C_{max}$ ( $\mu\text{g/mL}$ ) <sup>a)</sup>	$AUC_{0-28h}$ ( $\mu\text{g}^*\text{h/mL}$ ) <sup>a)</sup>
Lys, NaCMC, and FE	Formulation	$18.24 \pm 3.41$ <sup>b)</sup>	$144.09 \pm 35.89$
	Physical mixture	$13.25 \pm 3.90$	$129.91 \pm 28.23$
Meg, NaCMC, and FE	Formulation	$16.30 \pm 2.25$ <sup>b)</sup>	$140.09 \pm 37.83$ <sup>b)</sup>
	Physical mixture	$7.09 \pm 2.52$	$76.61 \pm 12.67$

a) Concentrations as fenofibric acid

b) Statistically different ( $p < 0.05$ ) compared to the corresponding physical mixture

#### 4. Discussion

The polymer selection in the development of a solid dispersion is a key factor for amorphous stability and beneficial drug supersaturation kinetics upon release. Such multiple functionality of an ideal polymer would call for selecting from a broad range of pharmaceutical polymers but there is unfortunately only a limited amount polymers available that are orally acceptable. Consequently, the development of new polymer matrices is needed but as new chemical entities, it would mean substantial work effort with regard to toxicological qualification and regulatory approval<sup>35</sup>. An interesting alternative approach is to target specific molecular interactions of small molecular additives that are already regulatory approved for the administration route with pharmaceutical polymers to obtain modified polymeric matrices<sup>26</sup>. Such an approach bears the potential to customize polymeric matrices, for example regarding stability, a manufacturing process or a release profile.

A recently published article from our research group highlighted the beneficial properties of the two additives, Meg and Lys, on the processability of the polyelectrolyte NaCMC. These additives enabled HME processing of the otherwise high melting/degrading polyelectrolyte, NaCMC, resulting in a homogenous glass<sup>25</sup>. The present research used the drug FE as a model compound to investigate these polyelectrolyte matrices *in vitro* as well as *in vivo* to assess their biopharmaceutical performance.

FE could be incorporated at a concentration of 7.5 % (w/w), which was determined as the stable amorphous drug load in the formulation. In such low drug loadings the polymer plays an important role in the release in a way that liquid-liquid phase separation and drug enrichment on the polymeric surface can be neglected,

which otherwise may have a negative impact on the dissolution performance<sup>36</sup>. Therefore, the effects of the modified matrix with its hydration kinetics and molecular interaction with drug were expected to dominate biopharmaceutical performance.

The dissolution curves in the current study highlighted, how different polymeric matrices impact the release and supersaturation behavior of FE. The delayed release in the dissolution curve of the Lys as well as the Meg extrudate may be explained by an increase in viscosity by NaCMC as expected for this polyelectrolyte<sup>34</sup>.

Moreover, Lys as a highly water-soluble amino acid with protonated amines in water can form both ionic interactions with NaCMC as well as exhibit likely hydrogen bonding with the drug. Meg as co-former would interact via hydrogen bonding with NaCMC and although there is no charge upon aqueous dispersion, there is still the possibility to exhibit some hydrogen bonding with FE.

The highly soluble amino acid as co-former led to a modified polyelectrolyte matrix that greatly enhanced the maximum drug supersaturation and could sustain it over a sufficiently long time to alter the effective drug absorption. While the present research had a focus on modification of the polymer matrix, the use of highly soluble amino acids has been suggested before in other co-amorphous systems where the primary goal was the interaction of drug and co-former to target increased amorphous stability<sup>37</sup>.

The existence of different relevant molecular interactions were in agreement with FTIR spectroscopic results of both systems. In particular, the O-H and N-H stretching vibration of Meg were broadened in the extrudate, which could be interpreted as a less defined structure as a result of hydrogen bonding between Meg and the other molecules (Figure 5). Meg was proven to be able to form such hydrogen bonds<sup>38,39</sup>. These findings were in line with the molecular dynamics simulation, which indicated a dense network of hydrogen bonds between the additive and NaCMC. However, the simulation also suggested that FE was located on the surface rather than in the polymeric bulk of the system with Meg, which may also have translated into different stabilization of supersaturated drug upon aqueous dispersion (Figure 2).

The FTIR pattern of the Lys formulation highlighted the interaction between the additive and NaCMC, in accordance with what was reported for the amino acid and a comparable substance in a previous study<sup>40</sup>.

Although the molecular simulation was of a qualitative nature to obtain an atomistic visualization of the simplified systems, it suggested that FE was well embedded in the modified matrix (Figure 1) while the drug could not integrate so well into the polymeric matrix of the co-former Meg (Figure 1 and 2). Such molecular integration and stronger matrix interaction may result in superior stabilization in the solid as well as in the solubilized form of the drug (Figure 7)<sup>41</sup>. The utility of molecular dynamics simulations and docking has previously been shown to be helpful in the evaluation of solid dispersion formulations and

depending on the simulation details, qualitative or even quantitative predictions may be obtained<sup>42</sup>. While the ionic moieties of a polymer are especially important for its swelling in aqueous media, the interactions with a poorly soluble drug are often complex. An example is that even though ionic and polar interactions are more energetic than weaker Van der Waals interactions, the latter can in their summation result in a substantial contribution to how drug attaches to a polymer upon aqueous dispersion<sup>43,44</sup>.

The dissolution profile of the Lys/NaCMC/FE formulation in contrast to the physical mixture underlined the stabilization properties of the polyelectrolyte matrix for the supersaturated state of FE. An initial high concentration of the physical mixture may have been caused by some surface amorphization during drug mixing or a direct excipient effect on solubilization. However, concentrations decreased rapidly to the saturation level, which was in contrast to the extruded formulation that was able to stabilize the supersaturated FE concentration over the time of the experiment. As such stabilization of supersaturated drug, another mechanism than the direct interaction within the polyelectrolyte matrix for the stabilization of the supersaturation is the increase in viscosity through NaCMC<sup>45</sup>. This could be a more general effect of a fast swelling polyelectrolyte and the viscosity measurements between the different samples showed barely differences except for slightly lower values for the physical mixture of the system with Meg (Table 6.1). The *in vitro* and the *in vivo* experiments were compatible with the NaCMC viscosity increase that may have led to some lag-time in release as well as it may have affected drug supersaturation. This would be in line with previous experiments investigating the influence of polymeric mixtures on the release<sup>34</sup> and the viscosity increase during aqueous dispersion through NaCMC<sup>46</sup>.

In comparison, the amorphous formulations showed higher exposure in the rat study than their corresponding physical mixtures (Figure 9). Although the Lys formulation did show an increasing trend in  $AUC_{0-28h}$  compared to the physical mixture, this increase was not statistically significant. However, the  $C_{max}$  was significantly increased in comparison to the physical mixture (Table 2). The comparatively good performance of the crystalline FE in combination with lysine and NaCMC was likely due to specific effects of the polyelectrolyte matrix combined with more general drug solubilization through phospholipids and bile salts<sup>47</sup>. Given these interesting result of the lysine physical mixture, more research can in the future also investigate the biopharmaceutical potential of crystalline formulations with polyelectrolytes and co-formers to enhance oral absorption.

The Meg formulation showed a faster release with a lower degree drug of supersaturation *in vitro* and was able to yield a significantly higher AUC and  $C_{max}$  when compared to its physical mixture. As for the *in vivo* comparison, the highest AUC and  $C_{max}$  were reported for the Lys formulation, which was in line with the *in vitro* dissolution experiments. Therefore, the obtained results were encouraging to use a modified polyelectrolyte matrix for the solubility and bioavailability enhancement of poorly water-soluble drugs.



## 5. Conclusion

Amorphous formulations have become a key method to increase the absorption of poorly water-soluble drugs. A limitation was, however, the selection of polymer because it has to fulfill different functionalities in the manufacturing of the formulation, for stability on the shelf as well regarding biopharmaceutical performance. This was addressed by the concept of modified polymeric matrices and the present study showed that addition of Lys and Meg enabled the amorphous formulation of FE in a new NaCMC polyelectrolyte matrix. The *in vitro* and *in vivo* results suggested advantages of the amorphous formulations compared to the physical mixture references. The amorphous formulations had significantly higher  $C_{max}$  values than their corresponding physical mixtures, which was in line with the dissolution experiments. This study presents the *in vivo* study of the previously developed polyelectrolyte matrices<sup>25</sup>. The promising results show the potential of polyelectrolytes to enable supersaturating oral drug delivery. Future research on ASDs containing polyelectrolytes as a modified matrix for HME is needed to further investigate the specific advantages for a broad range of poorly water-soluble drugs.

### Declarations

### Conflict of interest

The authors declare that they have no conflicts of interest to disclose.

### Funding

This project has received funding from the European Union's Horizon 2020 Research and Innovation Program under grant agreement No 674909.

### Literature

- (1) Gupta, P.; Chawla, G.; Bansal, A. K. Physical Stability and Solubility Advantage from Amorphous Celecoxib: The Role of Thermodynamic Quantities and Molecular Mobility. *Mol. Pharm.* **2004**, *1* (6), 406–413.
- (2) Taylor, L. S.; Zhang, G. G. Z. Physical Chemistry of Supersaturated Solutions and Implications for Oral Absorption. *Adv. Drug Deliv. Rev.* **2016**, *101*, 122–142.
- (3) Dahan, A.; Beig, A.; Lindley, D.; Miller, J. M. The Solubility–Permeability Interplay and Oral

- Drug Formulation Design: Two Heads Are Better than One. *Adv. Drug Deliv. Rev.* **2016**, *101*, 99–107.
- (4) Buckley, S. T.; Frank, K. J.; Fricker, G.; Brandl, M. Biopharmaceutical Classification of Poorly Soluble Drugs with Respect to “Enabling Formulations.” *European Journal of Pharmaceutical Sciences*. 2013.
  - (5) Galia, E.; Nicolaides, E.; Hörter, D.; Löbenberg, R.; Reppas, C.; Dressman, J. B. Evaluation of Various Dissolution Media for Predicting in Vivo Performance of Class I and II Drugs. *Pharm. Res.* **1998**, *15* (5), 698–705.
  - (6) Dressman, J. B.; Amidon, G. L.; Reppas, C.; Shah, V. P. Dissolution Testing as a Prognostic Tool for Oral Drug Absorption: Immediate Release Dosage Forms. *Pharm. Res.* **1998**, *15* (1), 11–22.
  - (7) Vertzoni, M.; Fotaki, N.; Nicolaides, E.; Reppas, C.; Kostewicz, E.; Stippler, E.; Leuner, C.; Dressman, J. Dissolution Media Simulating the Intraluminal Composition of the Small Intestine: Physiological Issues and Practical Aspects. *J. Pharm. Pharmacol.* **2004**, *56* (4), 453–462.
  - (8) Kawakami, K. Crystallization Tendency of Pharmaceutical Glasses: Relevance to Compound Properties, Impact of Formulation Process, and Implications for Design of Amorphous Solid Dispersions. *Pharmaceutics* **2019**, *11* (5), 202.
  - (9) Hancock, B. C.; Parks, M. What Is the True Solubility Advantage for Amorphous Pharmaceuticals? *Pharm. Res.* **2000**, *17* (4), 397–404.
  - (10) Wyttenbach, N.; Janas, C.; Siam, M.; Lauer, M. E.; Jacob, L.; Scheubel, E.; Page, S. Miniaturized Screening of Polymers for Amorphous Drug Stabilization (SPADS): Rapid Assessment of Solid Dispersion Systems. *Eur. J. Pharm. Biopharm.* **2013**, *84* (3), 583–598.
  - (11) Price, D. J.; Ditzinger, F.; Koehl, N. J.; Jankovic, S.; Tsakiridou, G.; Nair, A.; Holm, R.; Kuentz, M.; Dressman, J. B.; Saal, C. Approaches to Increase Mechanistic Understanding and Aid in the Selection of Precipitation Inhibitors for Supersaturating Formulations - a PEARRL Review. *J. Pharm. Pharmacol.* **2019**, *71* (4), 483–509.
  - (12) Patel, D. D.; Anderson, B. D. Effect of Precipitation Inhibitors on Indomethacin Supersaturation Maintenance: Mechanisms and Modeling. *Mol. Pharm.* **2014**, *11* (5), 1489–1499.
  - (13) Chavan, R. B.; Thipparaboina, R.; Kumar, D.; Shastri, N. R. Evaluation of the Inhibitory Potential

- of HPMC, PVP and HPC Polymers on Nucleation and Crystal Growth. *RSC Adv.* **2016**, *6* (81), 77569–77576.
- (14) Price, D. J.; Nair, A.; Kuentz, M.; Dressman, J.; Saal, C. Calculation of Drug-Polymer Mixing Enthalpy as a New Screening Method of Precipitation Inhibitors for Supersaturating Pharmaceutical Formulations. *Eur. J. Pharm. Sci.* **2019**, *132*, 142–156.
- (15) Williams, H. D.; Trevaskis, N. L.; Charman, S. A.; Shanker, R. M.; Charman, W. N.; Pouton, C. W.; Porter, C. J. H. Strategies to Address Low Drug Solubility in Discovery and Development. *Pharmacol. Rev.* **2013**, *65* (1), 315–499.
- (16) Stoimenovski, J.; MacFarlane, D. R.; Bica, K.; Rogers, R. D. Crystalline vs. Ionic Liquid Salt Forms of Active Pharmaceutical Ingredients: A Position Paper. *Pharm. Res.* **2010**, *27* (4), 521–526.
- (17) Barmapalexis, P.; Syllignaki, P.; Kachrimanis, K. A Study of Water Uptake by Selected Superdisintegrants from the Sub-Molecular to the Particulate Level. *Pharm. Dev. Technol.* **2018**, *23* (5), 476–487.
- (18) Moser, K.; Kriwet, K.; Kalia, Y. N.; Guy, R. H. Stabilization of Supersaturated Solutions of a Lipophilic Drug for Dermal Delivery. *Int. J. Pharm.* **2001**, *224* (1–2), 169–176.
- (19) Newman, A.; Knipp, G.; Zografu, G. Assessing the Performance of Amorphous Solid Dispersions. *J. Pharm. Sci.* **2012**, *101* (4), 1355–1377.
- (20) Hancock, B. C.; Shamblin, S. L.; Zografu, G. Molecular Mobility of Amorphous Pharmaceutical Solids Below Their Glass Transition Temperatures. *Pharm. Res. An Off. J. Am. Assoc. Pharm. Sci.* **1995**.
- (21) Chokshi, R. J.; Shah, N. H.; Sandhu, H. K.; Malick, A. W.; Zia, H. Stabilization of Low Glass Transition Temperature Indomethacin Formulations: Impact of Polymer-Type and Its Concentration. *J. Pharm. Sci.* **2008**, *97* (6), 2286–2298.
- (22) Edueng, K.; Mahlin, D.; Bergström, C. A. S. The Need for Restructuring the Disordered Science of Amorphous Drug Formulations. *Pharm. Res.* **2017**, *34* (9), 1754–1772.
- (23) Rowe, R. C.; Sheskey, P. J.; Fenton, M. E. Handbook Of Pharmaceutical Excipients: Pharmaceutical Excipients. In *American Pharmacists Association*; Washington D.C., USA, 2012.

- (24) Newman, A.; Reutzel-Edens, S. M.; Zografi, G. Coamorphous Active Pharmaceutical Ingredient–Small Molecule Mixtures: Considerations in the Choice of Coformers for Enhancing Dissolution and Oral Bioavailability. *J. Pharm. Sci.* **2018**, *107* (1), 5–17.
- (25) Ditzinger, F.; Dejoie, C.; Sisak Jung, D.; Kuentz, M. Polyelectrolytes in Hot Melt Extrusion: A Combined Solvent-Based and Interacting Additive Technique for Solid Dispersions. *Pharmaceutics* **2019**, *11* (4), 174.
- (26) Ditzinger, F.; Scherer, U.; Schönenberger, M.; Holm, R.; Kuentz, M. Modified Polymer Matrix in Pharmaceutical Hot Melt Extrusion by Molecular Interactions with a Carboxylic Coformer. *Mol. Pharm.* **2019**, *16* (1), 141–150.
- (27) Bevernage, J.; Forier, T.; Brouwers, J.; Tack, J.; Annaert, P.; Augustijns, P. Excipient-Mediated Supersaturation Stabilization in Human Intestinal Fluids. *Mol. Pharm.* **2011**, *8* (2), 564–570.
- (28) Berthelsen, R.; Holm, R.; Jacobsen, J.; Kristensen, J.; Abrahamsson, B.; Müllertz, A. Kolliphor Surfactants Affect Solubilization and Bioavailability of Fenofibrate. Studies of in Vitro Digestion and Absorption in Rats. *Mol. Pharm.* **2015**, *12* (4), 1062–1071.
- (29) Negrini, R.; Aleandri, S.; Kuentz, M. Study of Rheology and Polymer Adsorption Onto Drug Nanoparticles in Pharmaceutical Suspensions Produced by Nanomilling. *J. Pharm. Sci.* **2017**, *106* (11), 3395–3401.
- (30) Krieger, E.; Vriend, G. YASARA View – Molecular Graphics for All Devices from Smartphones to Work Stations. *Bioinformatics* **2014**, *30* (20), 2981–2982.
- (31) Bragg, W. L. Diffraction of Short Electromagnetic Waves by a Crystal. *Proc. Camb. Philol. Soc.* **1913**, *17*, 43–57.
- (32) Do, T. T.; Van Speybroeck, M.; Mols, R.; Annaert, P.; Martens, J.; Van Humbeeck, J.; Vermant, J.; Augustijns, P.; Van den Mooter, G. The Conflict between in Vitro Release Studies in Human Biorelevant Media and the in Vivo Exposure in Rats of the Lipophilic Compound Fenofibrate. *Int. J. Pharm.* **2011**, *414* (1–2), 118–124.
- (33) Fagerberg, J. H.; Karlsson, E.; Ulander, J.; Hanisch, G.; Bergström, C. A. S. Computational Prediction of Drug Solubility in Fasted Simulated and Aspirated Human Intestinal Fluid. *Pharm. Res.* **2015**, *32* (2), 578–589.

- (34) Kalivoda, A.; Fischbach, M.; Kleinebudde, P. Application of Mixtures of Polymeric Carriers for Dissolution Enhancement of Fenofibrate Using Hot-Melt Extrusion. *Int. J. Pharm.* **2012**, *429* (1–2), 58–68.
- (35) Elder, D. P.; Kuentz, M.; Holm, R. Pharmaceutical Excipients — Quality, Regulatory and Biopharmaceutical Considerations. *Eur. J. Pharm. Sci.* **2016**, *87*, 88–99.
- (36) Saboo, S.; Mugheirbi, N. A.; Zemlyanov, D. Y.; Kestur, U. S.; Taylor, L. S. Congruent Release of Drug and Polymer: A “Sweet Spot” in the Dissolution of Amorphous Solid Dispersions. *J. Control. Release* **2019**, *298*, 68–82.
- (37) Kasten, G.; Nouri, K.; Grohgan, H.; Rades, T.; Löbmann, K. Performance Comparison between Crystalline and Co-Amorphous Salts of Indomethacin-Lysine. *Int. J. Pharm.* **2017**, *533* (1), 138–144.
- (38) Telang, C.; Mujumdar, S.; Mathew, M. Improved Physical Stability of Amorphous State through Acid Base Interactions. *J. Pharm. Sci.* **2009**, *98* (6), 2149–2159.
- (39) Liu, X.; Zhou, L.; Zhang, F. Reactive Melt Extrusion To Improve the Dissolution Performance and Physical Stability of Naproxen Amorphous Solid Dispersions. *Mol. Pharm.* **2017**, *14* (3), 658–673.
- (40) Laitinen, R.; Löbmann, K.; Grohgan, H.; Strachan, C.; Rades, T. Amino Acids as Co-Amorphous Excipients for Simvastatin and Glibenclamide: Physical Properties and Stability. *Mol. Pharm.* **2014**, *11* (7), 2381–2389.
- (41) Edueng, K.; Mahlin, D.; Larsson, P.; Bergström, C. A. S. Mechanism-Based Selection of Stabilization Strategy for Amorphous Formulations: Insights into Crystallization Pathways. *J. Control. Release* **2017**, *256*, 193–202.
- (42) Barmpalexis, P.; Karagianni, A.; Katopodis, K.; Vardaka, E.; Kachrimanis, K. Molecular Modelling and Simulation of Fusion-Based Amorphous Drug Dispersions in Polymer/Plasticizer Blends. *Eur. J. Pharm. Sci.* **2019**, *130*, 260–268.
- (43) Saal, W.; Ross, A.; Wyttenbach, N.; Alsenz, J.; Kuentz, M. Unexpected Solubility Enhancement of Drug Bases in the Presence of a Dimethylaminoethyl Methacrylate Copolymer. *Mol. Pharm.* **2018**, *15* (1), 186–192.

- (44) Saal, W.; Wytttenbach, N.; Alsenz, J.; Kuentz, M. Interactions of Dimethylaminoethyl Methacrylate Copolymer with Non-Acidic Drugs Demonstrated High Solubilization in Vitro and Pronounced Sustained Release in Vivo. *Eur. J. Pharm. Biopharm.* **2018**, *125*, 68–75.
- (45) Warren, D. B.; Benameur, H.; Porter, C. J. H.; Pouton, C. W. Using Polymeric Precipitation Inhibitors to Improve the Absorption of Poorly Water-Soluble Drugs: A Mechanistic Basis for Utility. *J. Drug Target.* **2010**, *18* (10), 704–731.
- (46) Barbucci, R.; Magnani, A.; Consumi, M. Swelling Behavior of Carboxymethylcellulose Hydrogels in Relation to Cross-Linking, PH, and Charge Density. *Macromolecules* **2000**, *33* (20), 7475–7480.
- (47) Schwebel, H. J.; van Hoogevest, P.; Leigh, M. L. S.; Kuentz, M. The Apparent Solubilizing Capacity of Simulated Intestinal Fluids for Poorly Water-Soluble Drugs. *Pharm. Dev. Technol.* **2011**, *16* (3), 278–286.